Numerical Investigation of Carbon Braided Composites at the Mesoscale: using Computer Tomography as a Validation Tool

Mathieu Vinot[1], Martin Holzapfel[1], Raouf Jemmali[1]

[1] Institute of Structures and Design, German Aerospace Center, Stuttgart

Keywords: braided composites, mesoscopic scale, computer-tomography, TexGen

Abstract

Analytical and numerical approaches have been limited in their ability to predict the properties of braided composites because of the high complexity of the roving architecture within the textile. While many analytical theories have been developed to determinate the stiffness of braided composites, only few models have tried to reproduce their behaviour up to and after the global failure. A finite element (FE) approach has been developed in the present study to predict the mechanical properties of braided composites. The numerical material characterisation relies on the generation of an idealised geometrical model using the open-source software TexGen, which constitutes the starting point for further finite-element simulations. The validation of the geometry and its deformations under load is then performed based on a Computer Tomography (CT) investigation on a braided tensile test specimen.

The numerical model of a 60°-biaxial braid appears to be in good agreement with the rovings' structure captured in the CT scans. It has been proven that simulating the compaction of the dry rovings results in a more accurate representation of the rovings' interlacing in the braided textile. Non-destructive technology, the CT scan furthermore allows for a detailed study of the failure modes within the braided structure.

This paper illustrates the modelling and validation process of a 60°-biaxial braided composite.

1 Introduction

Due to an increasing need to reduce weight, in the first place for racing or luxury cars, the use of composite materials strongly increased in the automotive industry over the past decades and has been extended to mid-range cars. Offering a high manufacturability with reduced production time and cost, braiding processes appear to be an efficient way of producing profile structures. In comparison to more classical composite types like non-crimp fabrics or weaves, braided composites present a complex roving interlacing which depends on process parameters and affects the numerical simulation of these structures.

As part of the research campus ARENA2036 [1], which groups together partners from the industry and research facilities, the DigitPro (Digital Prototype) project aims to develop a closed process chain for the manufacturing of braided composite parts including, amongst others, braiding, draping and infiltration simulations as well as virtual material tests (*Figure 1*). The validation of these numerical models is achieved through experimental material characterisation and structure tests in addition to the manufacturing of generic structures (*Figure 2*).

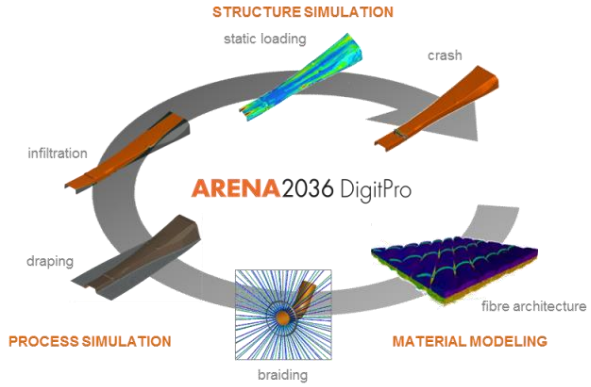

Figure 1: Process chain for braided textiles in the DigitPro project

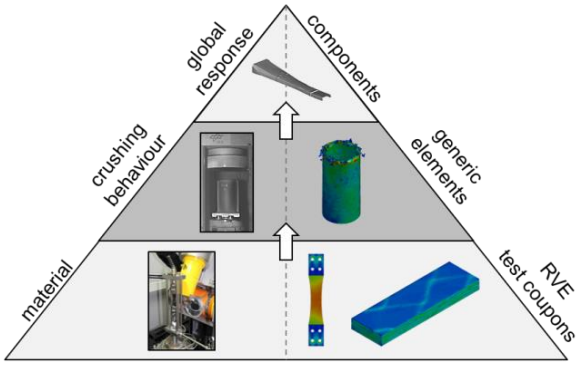

Figure 2: Test pyramid for the validation of numerical models

Several approaches have been investigated in the past to predict the stiffness and strengths of braided composites. The analytical model of Quek [2], modified by Shokrieh [3], successfully estimates the stiffness of different braid types using the classical laminate theory (CLT) and the principle of representative volume element (RVE). More recently, computer programs like TexGen have made it possible to model three-dimensional woven or braided composites for use in numerical analysis. However, numerical approaches need to be improved to accurately predict the braid's stiffness, strength and post-failure behaviour.

The presented work relies on the automated generation of a realistic braid's RVE for use in FE-simulations to predict the braid's behaviour. Using computer tomography and material tests, the predicted geometries and mechanical properties are validated.

2 Numerical simulation chain for braided composite

2.1 Modelling of a Representative Volume Element (RVE) with TexGen

The open-source software TexGen, developed at the University of Nottingham, and Python scripts are used to automatically model a three-dimensional, periodical RVE of the textile. The yarn centrelines are defined with a series of master nodes which are interpolated to form a one dimensional line. Yarn cross sections are represented as 2D shapes tangential to the yarn path. Based on experimental investigations, the yarn cross section is assumed to be elliptical and the major and minor axis can be measured on polished micrograph sections [4]. The yarn path and cross section geometry are then brought together to form the two-dimensional yarn surface. Detailed information about the modelling process is available in the software's documentation [5]. In the present case, the yarn geometry needs to be corrected to suppress the yarn penetrations. This step is carried out automatically by rotating the yarn cross sections or translating the master nodes. Finally, several layers are randomly stacked using a TexGen feature and meshed with the software TetGen (included in TexGen). The resulting braid geometry can be seen in *Figure 3*.

2.2 Compaction finite-element simulation

As shown in *Figure 3*, the initial TexGen geometry differs significantly from the real dry textile. By simulating the compaction process, which is actually performed under vacuum during the infiltration, the global fibre content and the yarn nesting are increased to reach realistic values. To this aim, the yarns are assigned an isotropic, elasto-plastic behaviour with a low yield stress (***MAT_024** in LS-DYNA). Thus, the yarns can experience high deformations without volume loss. The textile is compacted between two rigid plates (not represented in the figure), whose velocity is progressively increased after the initial contact to reduce contact instabilities [6]. The faces of the models are constrained using the command ***CONSTRAINED_NODE_SET** in tangential direction and periodic boundary conditions for opposite surfaces in normal direction (see 2.3.1). In case of a 60°-biaxial braid, the fibre content could be increased from 35% up to 54% (-11% of the experimental fibre content) during the compaction. The creation of the matrix mesh is performed in three steps after the compaction. Firstly, the RVE lateral surfaces are obtained by subtracting the yarn cross sections from the boundary planes. Then a closed triangle mesh is created by adding the yarn surface mesh to the boundary surface mesh. The result is finally used as a basis of a 3D tetrahedron model in TetGen.

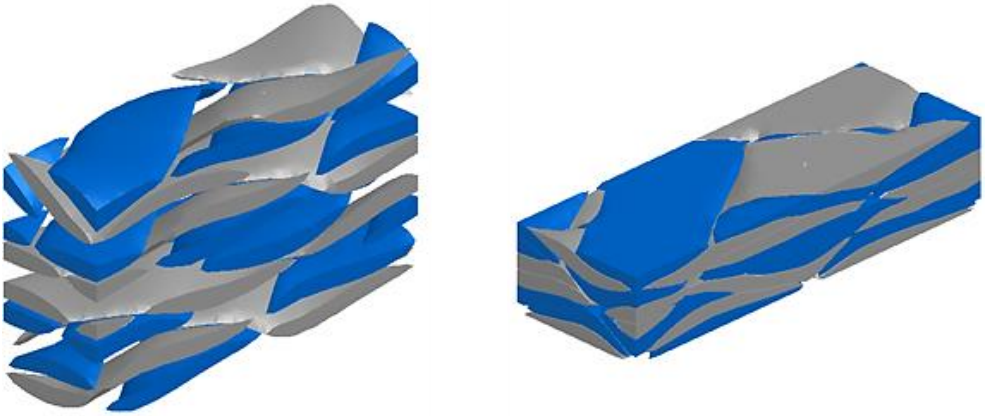

Figure 3: Dry fibres FE-model before (left) and after (right) the compaction

2.3 Simulation of the RVE under load

2.3.1 Periodic boundary conditions

Mesoscale simulations usually contain millions of degrees of freedom and require large amounts of computation time. To reduce the computational cost, periodic boundary conditions are implemented between two opposite faces to simulate the surrounding material [7]. This can be done in LS-DYNA by applying the command ***CONSTRAINED_MULTIPLE_GLOBAL** to a periodic mesh. The displacements of two opposite nodes (P_1 and P_2 in *Figure 4*) are coupled to the displacements of a master node M (equation 1), whose velocity is controlled during the simulation. Braid composites having a finite thickness, the surfaces facing in z-direction are not constrained using periodic boundary conditions.

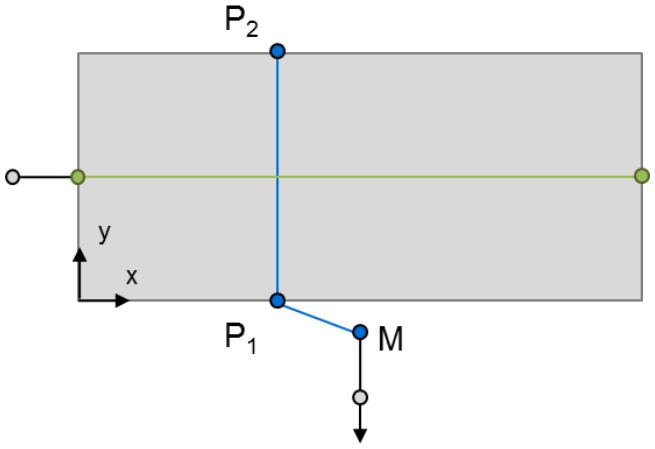

$$\begin{aligned} u_{x,M} + u_{x,P_1} - u_{x,P_2} &= 0 \\ u_{y,M} + u_{y,P_1} - u_{y,P_2} &= 0 \\ u_{z,M} + u_{z,P_1} - u_{z,P_2} &= 0 \end{aligned} \quad \textbf{(1)}$$

Figure 4: Implementation of the periodic boundary conditions in a RVE for a tensile load

2.3.2 Material models for HTS40 carbon rovings and RTM6 matrix

The braided composites simulated in this study are composed of HTS40 24k carbon rovings and RTM6 matrix. The material properties for the matrix are obtained from the manufacturer's datasheet. Very few material tests have been performed until now in the literature to investigate the material properties of impregnated carbon rovings. Chamis developed a method to estimate the elastic moduli and strengths of UD-composites using analytical formulae based on the classical laminate theory [8]. It must be remarked that the calculated transverse values are relatively conservative in comparison to the values from literature. The mechanical properties used for the dry carbon fibres and the yarn fibre content are based on estimations or on literature respectively [9].

The calculated values are further implemented in the **`*MAT_261`**. The material type **`*MAT_LAMINATED_FRACTURE_DAIMLER_PINHO`** is an orthotropic continuum damage model for laminated fibre-reinforced composites [10]. It implements fibre and matrix dominated failure mechanisms under tension and compression and a non-linear shear stress - shear strain curve can be attributed. In the longitudinal direction, the carbon rovings have a linear elastic behaviour up to failure (maximal stress criterion, equation 2). A coupled stress criterion is used for the transverse and shear load case (equation 3). In order to reduce numerical instabilities due to element erosion, damage in transverse tension and shear is defined with low fracture toughnesses. LS-DYNA automatically regularizes these values with the characteristic element length.

fibre failure under tension

$$e_f^2 = \left(\frac{\sigma_{11}}{X_t}\right)^2 - 1 \qquad \textbf{(2)}$$

matrix failure under tension and shear

$$e_m^2 = \left(\frac{\sigma_n}{Y_T}\right)^2 + \left(\frac{\sigma_T}{S_T}\right)^2 + \left(\frac{\sigma_L}{S_L}\right)^2 - 1 \qquad \textbf{(3)}$$

The matrix has an elasto-plastic behaviour and is modelled with the material type **`*MAT_PLASTICITY_COMPRESSION_TENSION`** (**`*MAT_124`**) in which two separate material curves for the tensile and the compressive domains are defined. A common failure strain under tension and compression is obtained from the material datasheet. Despite being originally designed to simulate the behaviour of metallic materials, this model is suited for the simulation of polymers as well, due to its simplicity and the low characterization effort required [11].
Normalized stress-strain curves for the material behaviours are given in *Figure 5*.

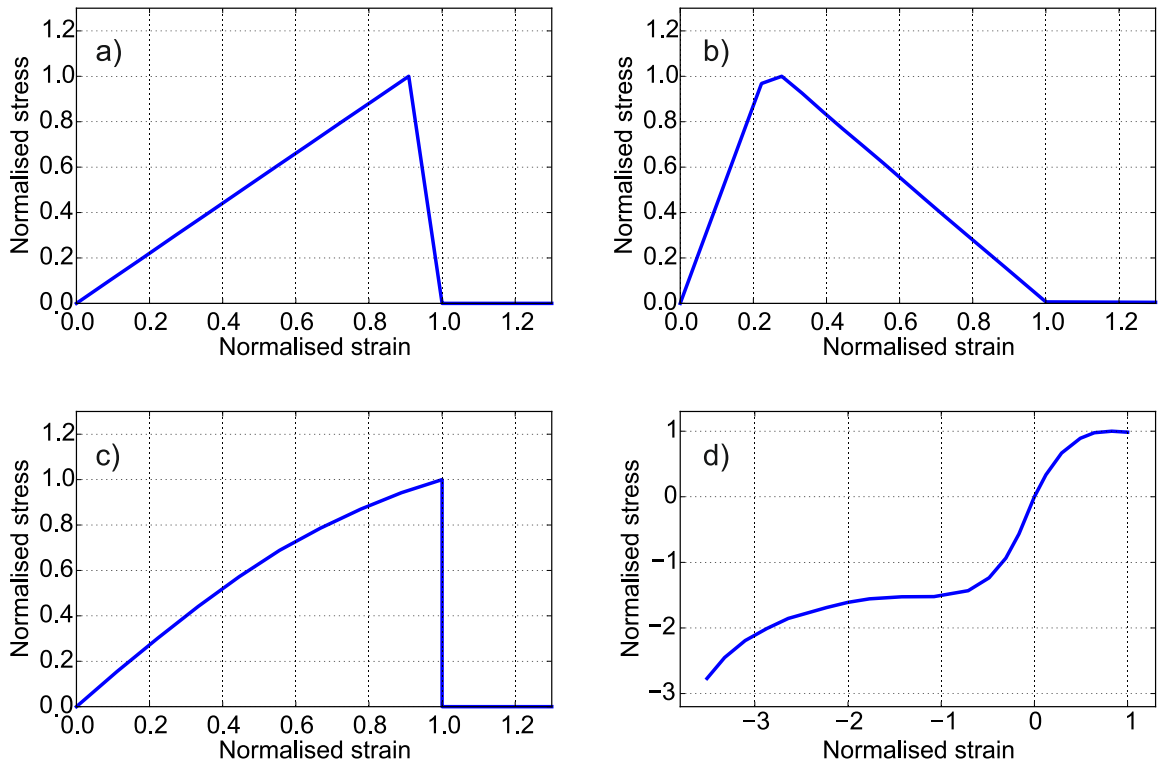

Figure 5: Normalised stress-strain curves for a) axial, b) transverse, c) shear roving behaviour and d) tension-compression matrix behaviour

2.3.3 Modelling approaches for the matrix-rovings interface

Several approaches can be used to model the interface between the rovings and the matrix. A direct modelling approach of this interface using cohesive elements is difficult due to the fibre geometry. Instead, the contact type ***CONTACT_AUTOMATIC_ONE_WAY_SURFACE_TO_SURFACE_TIEBREAK** with option 9 is used. This tiebreak contact, which forms an element-free equivalent of the material type ***MAT_138**, has an elastic behaviour and includes a bilinear traction-separation law with a quadratic mixed-mode delamination criterion and a damage formulation. The interface properties are chosen based on the work of Alfano [12].

2.3.4 RVE simulations

Explicit simulations under axial and transverse tension and under shear are performed to determine the mechanical properties of different braid types. The nodal force and the displacement of the master node are output to obtain the force-displacement curve.

Figure 6 displays the damage variable *dmat* within the unit cell at a global strain of 0.35% for the axial tension load case. High strains are primarily concentrated on the braid yarn's overlaps and propagate along the yarn in transverse direction. Cracks initiate at a strain of 0.46% under a combination of shear stresses and transverse stresses (*dmat* = 1). The first matrix failure between the rovings can be detected at a strain of 0.6% closely before the global failure. At 0.7% strain, global failure occurs in the 60°-oriented fibre bundles leading to a drop of 70% in the coupon's load. Afterwards, the textile is subjected to high deformations at a lower load level caused by the alignment of the rovings with the loading direction. The strain field in the unit cell still needs to be validated with in-situ CT-scans and optical strain measurements.

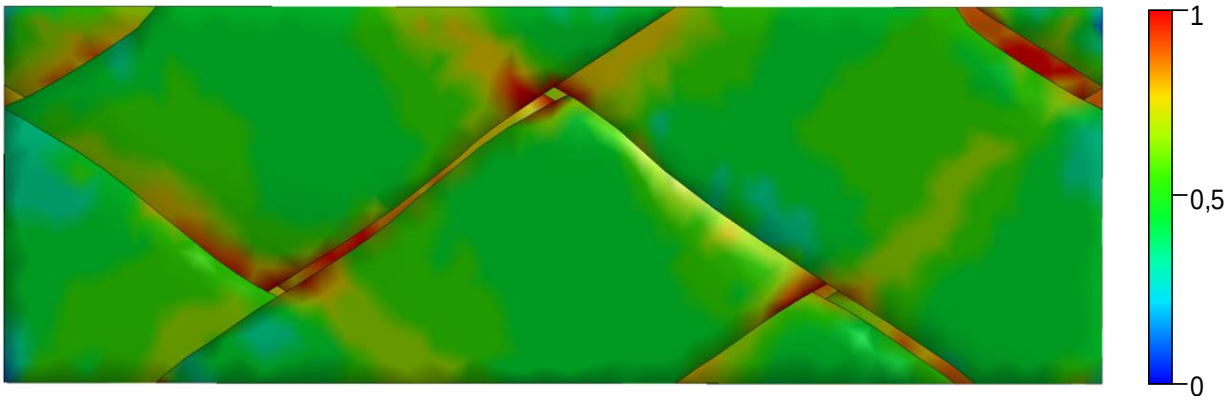

Figure 6: Predicted damage dmat (1 = failure reached) due to transverse and shear stresses in the rovings at a global strain of 0.35%

3 Experimental investigation of a 60°-biaxial carbon braid

To complement the RVE simulation, CT-scans are performed on 60°-biaxial carbon braided coupons to gain information about the yarn structure, the deformations under tensile loading and the failure mechanisms in braided textiles.

3.1 Experimental set-up

Investigating composite structures on the mesoscopic or microscopic scale with in-situ CT-scans requires the use of an apparatus that does not perturb the scanning process. An experimental set-up (*Figure 7*) was developed at the DLR, consisting mainly of a fixed frame in which a rotation-free tensile coupon is incrementally loaded [13]. The tensile load is measured with a 20 kN force sensor mounted on the frame. In this study, the load is increased in steps of 1 kN up to global failure and the narrowed centre section of 25 mm x 25 mm is scanned with a resolution of 15 µm.

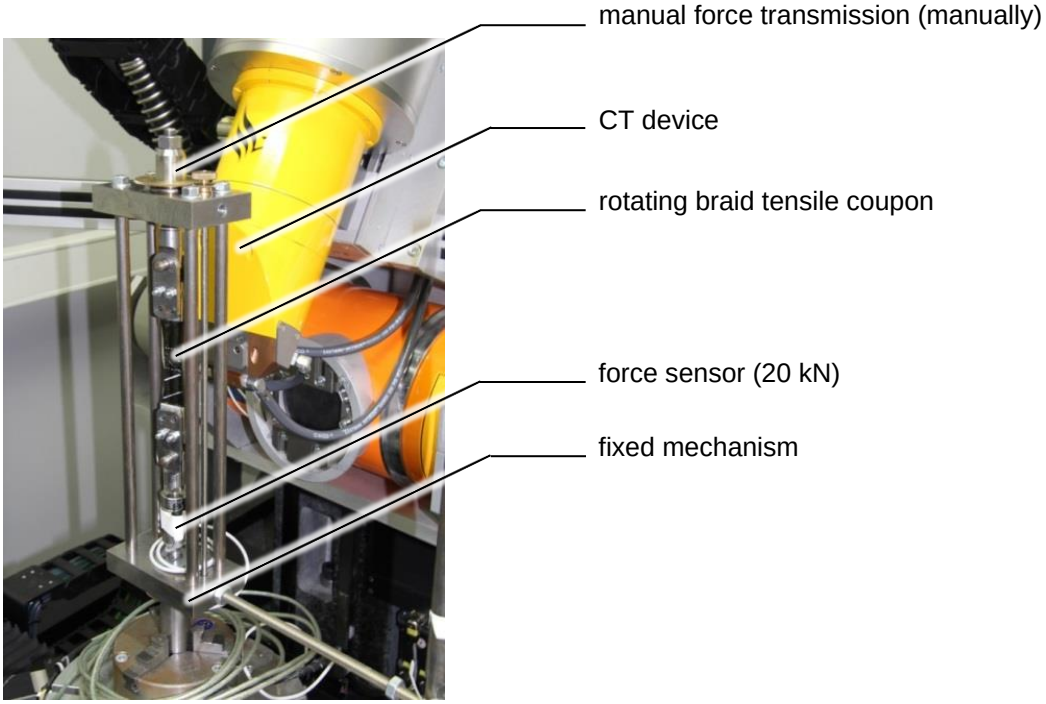

Figure 7: Experimental set-up for in-situ CT investigations

3.2 Results and validation of the simulation strategy

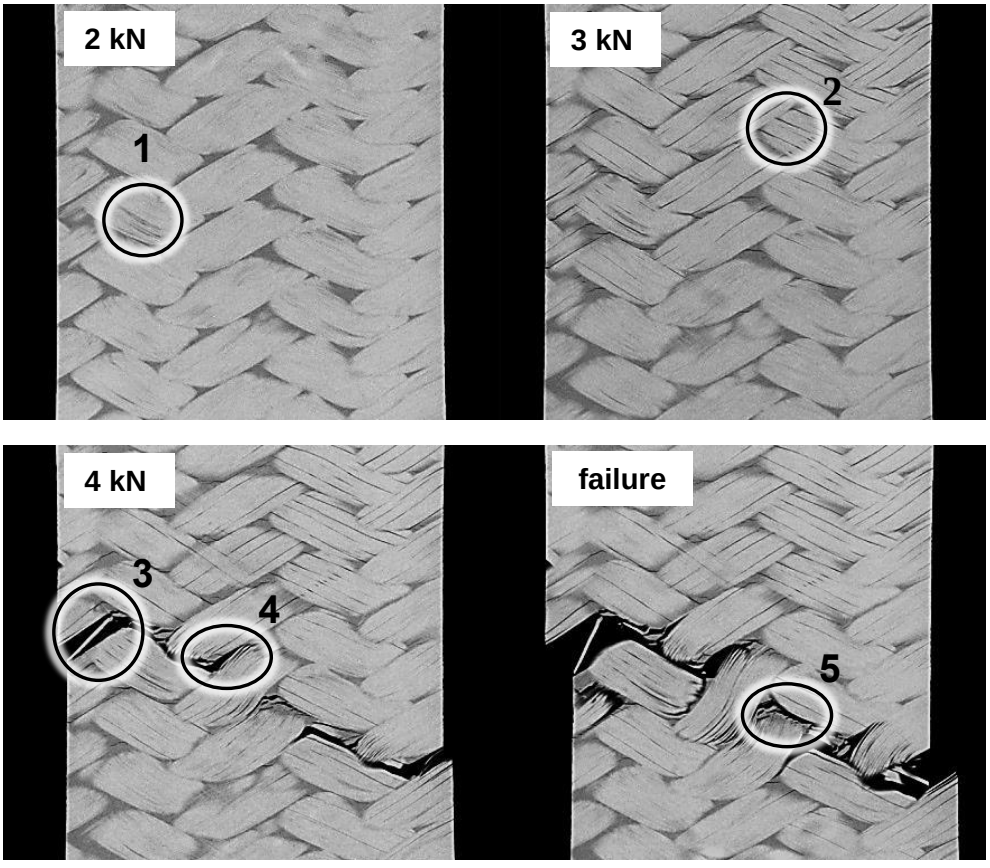

Figure 8: Deformation and failure of the 60°-biaxial braid under tensile load

At a resolution of 15 µm, the rovings are clearly defined and defects or voids (matrix-rich zones) in the yarns can be detected in the intact braid (1 in *Figure 8*). At a load of 3 kN, cracks grow in the rovings' longitudinal direction (2) and concentrate themselves around the flawed zones. After a phase of crack accumulation in the rovings, global failure is reached as cracks spread along the entire coupon's length along the yarns, at an angle of -60° to the loading direction. Failure occurs both as matrix failure in the rovings (3) and as matrix-roving debonding (4). A second load path is formed by the intact rovings in the 60° direction, leading to a fibre tensile failure (5).

Figure 9 and *Figure 10* show a good agreement between the simulated braid and the CT-scans. A high nesting of the rovings is reached in the simulated braid after its compaction.

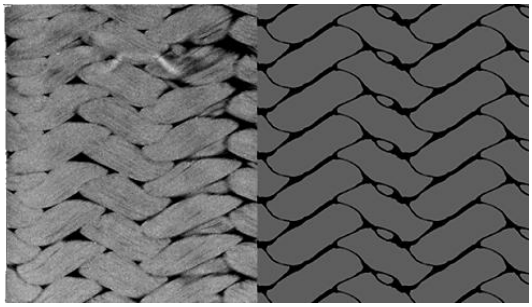

Figure 9: Comparison of the in-situ (left) and simulated (right) 60°-biaxial braid

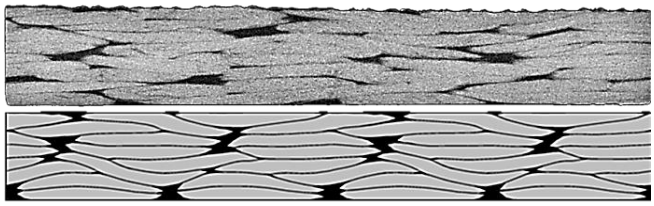

Figure 10: Comparison of the in-situ (top) and simulated (bottom) 60°-biaxial braid

Figure 11 shows the predicted response of the braid under tension in comparison with the experimental results. The FE-model provides a good estimation of the braid's global behaviour. The elasticity is close to the experiment at 10 GPa (95% of the measured value) and the failure values (strength of 67.8 MPa and failure strain of 0.71%) agree well with the measured mean values (*Table 1*). Furthermore, the post-failure behaviour has been predicted accurately. The simulation shows a brittle failure of the rovings in the 60°-direction (crack pattern in *Figure 12*) resulting in a second load path due to the intact -60°-oriented rovings. The discrepancy of the stiffness and strength values can be partly explained by the lower fibre content of the simulated braid in comparison to the experimental value.

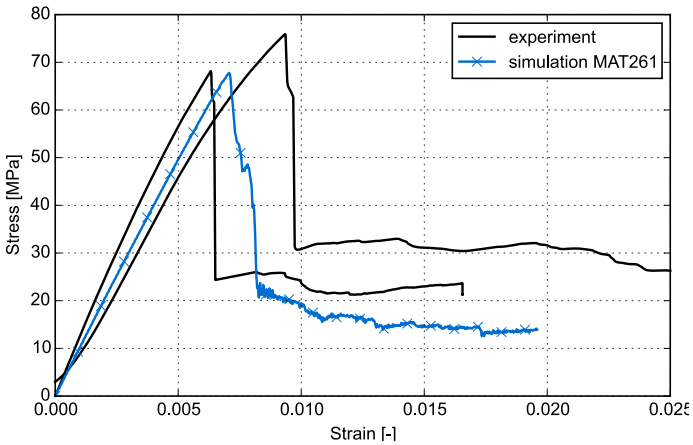

Figure 11: Simulated quasi-static response of a 60°-biaxial braid under tension compared to the experiment

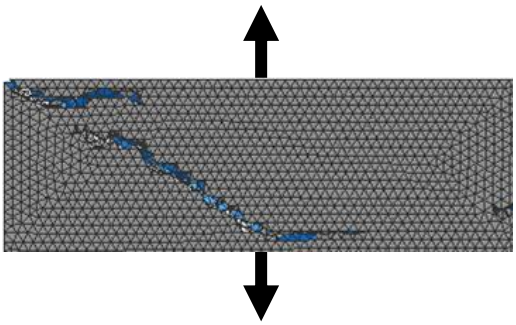

Figure 12: crack pattern in the simulated 60°-biaxial braid

	experiment	simulation
E_{11} [GPa]	10.5	10 (-5%)
σ_{11} [MPa]	72	67.8 (-6%)
ε_{11} [%]	0.77	0.71 (-8%)

Table 1: Comparison of the mechanical properties of a 60°-biaxial braid

4 Summary and outlook

It has been shown that the developed mesoscopic FE approach allows for a good prediction of the mechanical properties of a 60°-biaxial braid. By simulating the dry textile compaction, it was made possible to reproduce the nesting of the rovings in braided composites with very good accuracy, resulting in an improved prediction of the braid's behaviour. Nevertheless, focus has to be laid on the reliable determination of the transverse and shear roving's properties, which have a considerable effect on the braid's response. The present model must further be improved to take into account strain rate effects. From an experimental perspective, in-situ CT-scans offer an efficient way of investigating the fibre architecture of carbon braids and their behaviour under tension.
The simulation strategy must be validated using a wider range of biaxially and triaxially braided textiles. A multiscale strategy will be developed as part of the next project steps to transfer the mesoscopic properties to a macroscopic scale for the simulation of crash structures.

5 Literature

[1] http://www.arena2036.de/de/, 2. April 2015.

[2] S. Quek, A. Waas, K. Shawan and V. Agaram, "Analysis of 2D triaxial flat braided textile composites," *International Journal of Mechanical Sciences 45,* 2003.

[3] M. Shokrieh and M. Mazloomi, "An analytical method for calculating stiffness of two dimensional triaxial braided composites," *Composite Structures,* 2010.

[4] K. Birkefeld, "Virtuelle Optimierung von Geflecht-Preforms unter Berücksichtigung von Fertigungsaspekten," 2011.

[5] H. Lin, B. L.P. and A. C. Long, "Modelling and Simulating Textile Structures using TexGen," *Advances in Textile Engineering, Vol. 331, 44-47,* 2011.

[6] G. Grail, "Approche multimodèle pour la conception de structures composites à renfort tissé," 2013.

[7] J. D. Whitcomb, D. C. Clinton and T. Xiaodong, "Derivation of Boundary Conditions for Micromechanics Analyses of Plain and Satin Weave," *Journal of Composite Materials, vol. 34,* 2000.

[8] C. C. Chamis, "Mechanics of Composite Materials: Past, Present, and Future," 1984.

[9] J.W. Bull, "Numerical analysis and modelling of composite materials", 1996.

[10] S. Hartmann, "Neue Materialmodelle für Composites in LS-DYNA," 2013.

[11] A. Haufe, V. Effinger, P.Reithofer, M. Rollant, M. Fritz, „Validation and Material Modelling of Plastics", 2011.

[12] G. Alfano and M. A. Crisfield, "Finite element interface models for the delamination analysis of laminated composites: mechanical and computational issues," 2000.

[13] R. Jemmali, "Quantitative Bewertung von Verbundwerkstoffen auf der Basis von tomographischen Bildern," 2014.

Acknowledgement

This project is funded by the German Federal Ministry of Education and Research within the framework of the ARENA2036 project and managed by the Karlsruhe Institute of Technology.